PERGAMON

International Journal of Heat and Mass Transfer 41 (1998) 2799–2807

International Journal of HEAT and MASS TRANSFER

The developing Nusselt numbers for slug flow in rectangular ducts

M. Spiga[a]*, G. L Morini[b]

[a]*DIENCA, University of Bologna, Viale Risorgimento 2, 40136 Bologna, Italy*
[b]*Department of Engineering, University of Ferrara, Via Saragat 1, 44100 Ferrara, Italy*

Received 20 May 1997; in final form 22 September 1997

Abstract

A rigorous solution is obtained for the 3-D temperature field in the thermal entrance region of rectangular ducts, for Newtonian fluids in slug flow, with constant wall heat flux and fluid longitudinal heat flux (H2 boundary conditions). The solution is presented as a series of the transverse Cartesian co-ordinates, where the coefficients depend on both the longitudinal co-ordinate and the different combinations of heated and adiabatic walls. The thermal entrance lengths and the Nusselt numbers are calculated as functions of both the Graetz number and the aspect ratio. The temperature profiles, the thermal entrance lengths, and the Nusselt numbers are presented and discussed in tables and graphs.

Nomenclature

a, b longer and shorter sides, respectively, of the rectangular cross section [m]
D hydraulic diameter of the duct $2ab/(a+b)$ [m]
Gz Graetz number $D^2V/\zeta\alpha$
h heat transfer coefficient [W (m^2 K)$^{-1}$]
j, k, m, n summation indices
K fluid thermal conductivity [W (m K)$^{-1}$]
L_{th} dimensionless thermal entrance length
Nu Nusselt number hD/K
Nu^* fully established Nusselt number
P dimensionless heated perimeter length
q heat flux [W m^{-2}]
$T(\cdot)$ dimensionless fluid temperature
$T_b(\cdot)$ dimensionless fluid bulk temperature
$T_w(\cdot)$ dimensionless wall temperature
V fluid velocity [m s^{-1}]
x, y, z dimensionless rectangular Cartesian co-ordinates
z_{th} dimensionless longitudinal co-ordinate z/L_{th}.

Greek symbols
α fluid thermal diffusivity [m^2 s^{-1}]
β aspect ratio $b/a < 1$
$\theta(\cdot)$ fluid temperature [K]
θ_0 fluid inlet temperature [K]
ξ, ψ, ζ Cartesian co-ordinates [m].

1. Introduction

The heat transfer behaviour of flows in rectangular ducts is a topic of special interest in compact heat exchangers, such as radiators or condensers in air-conditioning units, as discussed in [1]. The rectangular geometry involves a more complex and arduous analysis rather than circular geometry, even for the simplest case of slug flow, which may approximate the actual flow of low Prandtl number fluids (where the hydrodynamic length is very much longer than the thermal entry length, so a uniform velocity profile can be assumed in the thermal entrance region). An investigation concerning the flow behaviour in the thermal entrance region of rectangular ducts requires a 3-D solution to predict the fluid temperature profile and the pertinent developing Nusselt numbers. The boundary conditions too, in rectangular ducts, become complex, because there are many possibilities to impose different temperatures or heat fluxes on the four wetted sides. The most interesting boundary

* Author to whom correspondence should be addressed.

0017–9310/98 $19.00
PII: S0017–9310(97)00352–9

condition, for its practical application, is the well known H2 condition, defined in [2], characterised by constant wall heat flux on the heated perimeter and constant fluid axial heat flux. Many different situations can be considered too, assuming a particular condition for every side of the rectangle. In literature eight classical H2 versions are proposed; they are symbolically specified as follows: 4 (four heated sides), 3L (three heated sides and one adiabatic short side), 3S (three heated sides and one adiabatic long side), 2L (two heated long sides and two adiabatic short sides), 2S (two heated short sides and two adiabatic long sides), 2C (one long and one short heated sides), 1L (one heated long side), 1S (one heated short side). The thermally developed flow has been object of several investigations, and the fully established Nusselt numbers for slug flow [3] and laminar flow [4] in H2 boundary conditions have been exhaustively published. On the contrary, the thermally developing Nusselt numbers for slug flow in H2 conditions are quoted in literature only for infinite parallel plates and square ducts. The same geometry, but with boundary conditions of the third kind, was considered in [5, 6]. A solution is presented in [7], concerning the developing Nusselt numbers (as a function of the Graetz number and the duct aspect ratio), but only for the 1L, 1S, 2L, and 2S versions.

The object of this work is to provide the 3-D fluid temperature profile in the thermal entry of rectangular ducts, with arbitrary aspect ratio for all the eight H2 boundary conditions. Then the developing Nusselt numbers and the thermal lengths are predicted by integrating temperature difference along the wetted perimeter of the rectangular cross section at different Graetz numbers. The theoretical model used in this paper is equivalent to the well studied 2-D transient heat conduction problem in a rectangular zone [8], the physical results constitute an original development in the field of basic thermal science and could provide a new tool for applications to engineering problems.

2. Basic equations and solution

Consider a steady laminar slug flow in the thermal entry length of a rectangular duct with uniform axial heat flux (the transverse velocity components and the effects of axial momentum and thermal diffusion are negligible). The hydrodynamic length is very much longer than the thermal entry length, hence a uniform velocity profile can be assumed in the thermal entrance region. A Cartesian system of co-ordinates ξ, ψ, ζ is assumed, with its origin in the left bottom corner of the inlet rectangular cross section (ψ along the short side b, ζ perpendicular to the cross section). The fluid has uniform velocity V and inlet temperature θ_0 ($\zeta = 0$). It is suitable introducing the dimensionless co-ordinates and temperature:

$$x = \frac{\xi}{a} \quad 0 \leqslant x \leqslant 1; \quad y = \frac{\psi}{a} \quad 0 \leqslant y \leqslant \beta = \frac{b}{a};$$

$$z = \frac{\zeta\alpha}{D^2 V} = \frac{1}{Gz} \quad z \geqslant 0; \quad T = \frac{K(\theta - \theta_0)}{qD}. \tag{1}$$

The fluid inlet condition is $T(x, y, 0) = 0$, while the H2 boundary conditions impose constant wall heat flux q on the heated perimeter, and adiabatic walls on the remaining part of the wetted perimeter:

$$\left.\frac{\partial T}{\partial x}\right|_{x=0} = d_1 \frac{(1+\beta)}{2\beta}, \quad \left.\frac{\partial T}{\partial x}\right|_{x=1} = d_2 \frac{(1+\beta)}{2\beta},$$

$$\left.\frac{\partial T}{\partial y}\right|_{y=0} = d_3 \frac{(1+\beta)}{2\beta}, \quad \left.\frac{\partial T}{\partial y}\right|_{y=\beta} = d_4 \frac{(1+\beta)}{2\beta} \tag{2}$$

where d_1, d_2, d_3, d_4 are reported in Table 1 for the eight versions of the H2 conditions.

The mathematical model is developed assuming, as usual, constant physical properties and neglecting axial conduction, power sources and natural convection. Consequently the dimensionless energy balance equation is readily obtained in the form:

$$\frac{\partial T}{\partial z} = \left(\frac{2\beta}{1+\beta}\right)^2 \left(\frac{\partial^2 T}{\partial x^2} + \frac{\partial^2 T}{\partial y^2}\right). \tag{3}$$

In order to solve equation (3), it proves convenient to take a double series of orthogonal functions:

$$T(x, y, z) = \sum_{n=0}^{\infty} \sum_{m=0}^{\infty} C_{nm}(z) \cos(n\pi x) \cos\left(m\pi \frac{y}{\beta}\right). \tag{4}$$

By substituting equation (4) in equation (3), multiplying each term by $\cos(k\pi x)\cos(j\pi y/\beta)$ and integrating over x and y, a simple equation can be obtained, considering that:

Table 1
Boundary condition coefficients

Version	d_1	d_2	d_3	d_4
1L	0	0	0 (or −1)	1 (or 0)
1S	0 (or −1)	1 (or 0)	0	0
2L	0	0	−1	1
2S	−1	1	0	0
2C	0 (or −1)	1 (or 0)	0 (or −1)	1 (or 0)
3L	0 (or −1)	1 (or 0)	−1	1
3S	−1	1	0 (or −1)	1 (or 0)
4	−1	1	−1	1

$$\int_0^{\beta}\int_0^1 \frac{\partial^2 T}{\partial x^2}\cos(k\pi x)\cos\left(j\pi\frac{y}{\beta}\right)\mathrm{d}x\,\mathrm{d}y = \begin{cases} -k^2\pi^2\dfrac{\beta}{4}C_{kj}(z) & \text{if } k\neq 0, j\neq 0 \\ 0 & \text{if } k=0, j\neq 0 \\ \dfrac{\pi^2\beta k^2}{2}(A_k - C_{k0}(z)) & \text{if } k\neq 0, j=0 \\ (d_2-d_1)\dfrac{1+\beta}{2\beta} & \text{if } k=0, j=0 \end{cases} \quad (5)$$

$$\int_0^{\beta}\int_0^1 \frac{\partial^2 T}{\partial y^2}\cos(k\pi x)\cos\left(j\pi\frac{y}{\beta}\right)\mathrm{d}x\,\mathrm{d}y = \begin{cases} -\dfrac{j^2\pi^2}{4\beta}C_{kj}(z) & \text{if } k\neq 0, j\neq 0 \\ \dfrac{\pi^2 j^2}{2\beta}(B_j - C_{0j}(z)) & \text{if } k=0, j\neq 0 \\ 0 & \text{if } k\neq 0, j=0 \\ (d_4-d_3)\dfrac{1+\beta}{2\beta} & \text{if } k=0, j=0 \end{cases} \quad (6)$$

$$\int_0^{\beta}\int_0^1 \frac{\partial T}{\partial z}\cos(k\pi x)\cos\left(j\pi\frac{y}{\beta}\right)\mathrm{d}x\,\mathrm{d}y = \begin{cases} \dfrac{\mathrm{d}C_{kj}}{\mathrm{d}z}\left(\dfrac{\beta}{4}\right) & \text{if } k\neq 0, j\neq 0 \\ \dfrac{\mathrm{d}C_{0j}}{\mathrm{d}z}\left(\dfrac{\beta}{2}\right) & \text{if } k=0, j\neq 0 \\ \dfrac{\mathrm{d}C_{k0}}{\mathrm{d}z}\left(\dfrac{\beta}{2}\right) & \text{if } k\neq 0, j=0 \\ \dfrac{\mathrm{d}C_{00}}{\mathrm{d}z}(\beta) & \text{if } k=0, j=0 \end{cases} \quad (7)$$

where the numbers A_k and B_j are inversely proportional to the square of the summation index:

$$A_k = [(-1)^k d_2 - d_1]\frac{1+\beta}{\pi^2\beta k^2} \qquad B_j = [(-1)^j d_4 - d_3]\frac{1+\beta}{\pi^2 j^2}. \quad (8)$$

Such a technique reduces the problem to a set of first order differential equations, containing the unknown coefficients $C_{kj}(z)$. The inlet condition ($T=0$ in $z=0$) provides an interesting result: due to the orthogonality of the cosinusoidal systems, all the coefficients $C_{kj}(z=0)$ must be identically 0. The other coefficients $C_{kj}(z)$ are easily obtained as the solution to the simple first order differential equations, linked to the boundary conditions; they are:

$$\begin{cases} C_{kj}(z) = 0 \\ \quad \text{if } k\neq 0, j\neq 0 \\ C_{k0}(z) = A_k\left[1-\exp\left(-\dfrac{4k^2\pi^2\beta^2}{(1+\beta)^2}z\right)\right] \\ \quad \text{if } k\neq 0, j=0 \\ C_{0j}(z) = B_j\left[1-\exp\left(-\dfrac{4j^2\pi^2}{(1+\beta)^2}z\right)\right] \\ \quad \text{if } k=0, j\neq 0 \\ C_{00}(z) = \dfrac{2L}{1+\beta}z \\ \quad \text{if } k=0, j=0 \end{cases} \quad (9)$$

The cancellation of the coefficients C_{kj} with $k\neq 0$, $j\neq 0$ allows to obtain the 3-D temperature distribution as the sum of a single series, with very fast convergence. The longitudinal co-ordinate appears only in exponential functions, while the transverse co-ordinate appear only in cosinusoidal functions; the final result reads as:

$$T(x,y,z) = \frac{2P}{1+\beta}z + \sum_{n=1}^{\infty} A_n\left[1-\exp\left(-\frac{4n^2\pi^2\beta^2}{(1+\beta)^2}z\right)\right]\cos(n\pi x) + B_n\left[1-\exp\left(-\frac{4n^2\pi^2}{(1+\beta)^2}z\right)\right]\cos\left(n\pi\frac{y}{\beta}\right). \quad (10)$$

By specifying the suitable coefficients (P, A_n, B_n), equation (10) provides the 3-D developing temperature profile in the rectangular cross section of the thermal entrance region for all the eight versions of the H2 boundary conditions.

3. Developing Nusselt numbers

For any cross section of the rectangular duct, the Nusselt number can be determined as a function of z, starting from the knowledge of the fluid bulk temperature and average wall temperature. From its definition the Nusselt number reads as:

$$Nu(z) = \frac{1}{T_w(z) - T_b(z)}. \quad (11)$$

Resorting to the temperature solution (10), the definitions of bulk temperature and wall temperature, given in [2], provide:

$$T_b(z) = \int_0^{\beta}\int_0^1 T(x,y,z)\,\mathrm{d}x\,\mathrm{d}y = \frac{2P}{(1+\beta)}z \quad (12)$$

$$T_w(z) = \frac{1}{P}\left(\int_0^{\beta}[d_2 T(1,y,z) - d_1 T(0,y,z)]\,dy + \int_0^{1}[d_4 T(x,\beta,z) - d_3 T(x,0,z)]\,dx\right). \quad (13)$$

To complete the investigation, the thermal entrance length L_{th} is calculated, as usual, by the numerical solution to the equation:

$$Nu(z = L_{th}) = 1.05\,Nu^* \quad (14)$$

where the fully established Nusselt number is well known in literature [3], and can be deduced too by equation (11) in the limit of $z \to \infty$ (corresponding to the fully developed region).

4. Results and discussion

The explicit analytical expression for the temperature profile, equation (10), has been processed for all the eight versions of the H2 boundary conditions in a very short time using a PC class computer. The introduction of dimensionless temperature and co-ordinates allows to obtain a 3-D distribution depending only on the duct aspect ratio. The illustrative examples reported in Figs. 1–4 refer to a flat rectangular duct ($\beta = 0.2$), for the 4, 3S, 3L, and 2C versions, with three different decreasing Graetz numbers (i.e. for increasing values of the longitudinal co-ordinate $z = 1/Gz$). As shown in Fig. 1, close to the fluid inlet section ($Gz = 100$), the four heated walls are responsible for a considerable increase in the wall temperature, mainly on the corners of the duct, while the bulk temperature remains very low. The short sides present higher temperatures than the long sides. When z increases ($Gz = 10$ and 1 in Fig. 1) the fluid temperature increases, arriving at the fully established profile. A similar trend is shown in Fig. 2, for the 3S version, where the long adiabatic side ($y = 0$) causes lower temperatures; the highest values occur on the two corners of the long heated side, the minimum at the centre of the long adiabatic wall. Figure 3 refers to the 3L version, the three heated walls give rise to a fluid temperature increase mainly on the corners of the short heated side, the opposite adiabatic short side keeps temperature at lower values. In Fig. 4 the temperature distribution is sketched for the 2C version, the two adjacent heated sides of the rectangle produces a considerable temperature increase, mostly on their mutual corner, the minimum value occurring on the opposite corner between the adiabatic sides.

For the 1S and 2S versions the coefficients B_n, equation (8), are identically zero, hence the temperature distribution is reduced to a 2-D profile depending only on x and z. Analogously the coefficients A_n are identically zero for the 1L and 2L versions, hence the pertinent temperature profiles do not depend on x. It is to point out

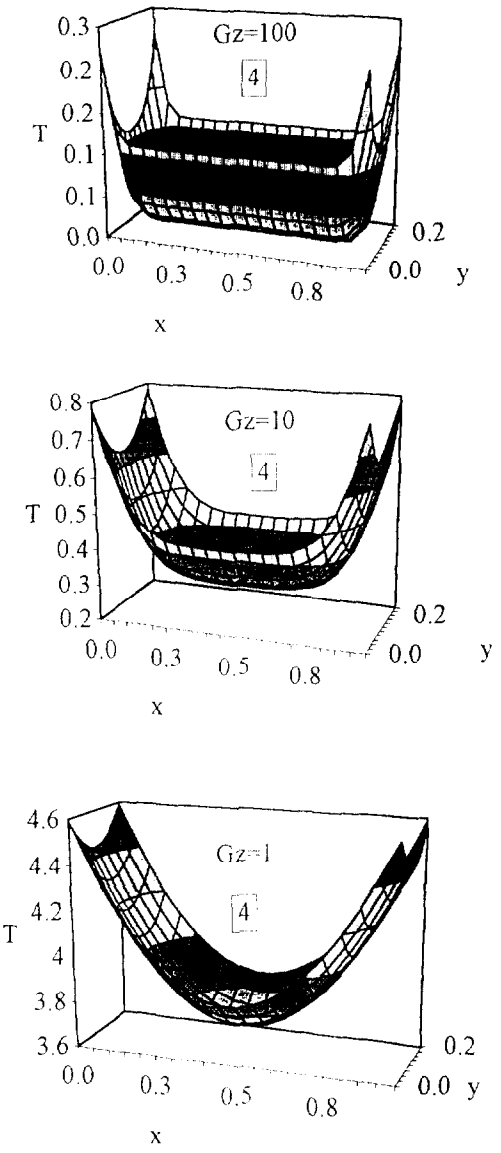

Fig. 1. Temperature distribution in the thermal entrance length, four heated walls.

that this behaviour is a peculiarity of the slug flow. In fact the fully developed temperature distribution for the 1S, 2S, 1L and 2L versions, in laminar fully developed flow with suitable spatial velocity profile, bears evidence of a dependence on both the co-ordinates x and y, as shown in the Figs. 4, 5, 7, and 8 of [4]. The semi-logarithmic diagrams of Figs. 5 and 6 refer to the 1S and 1L versions, respectively, for various values of the Graetz number; the heated side ($x = 1$ and $y = \beta = 0.2$, respectively) produces a sudden rise of the wall temperature while the temperature on the opposite side increases much more slowly. Figures 7 and 8 show the temperature dis-

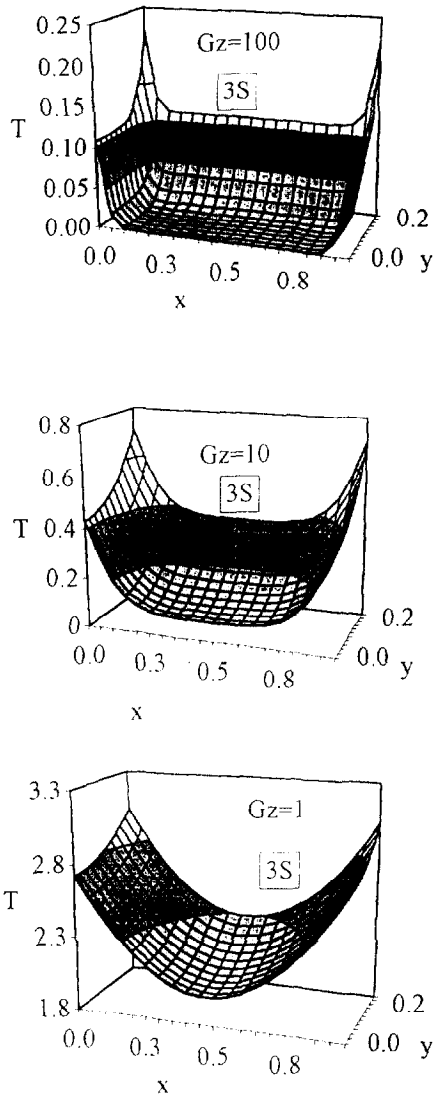

Fig. 2. Temperature distribution in the thermal entrance length, 3S version.

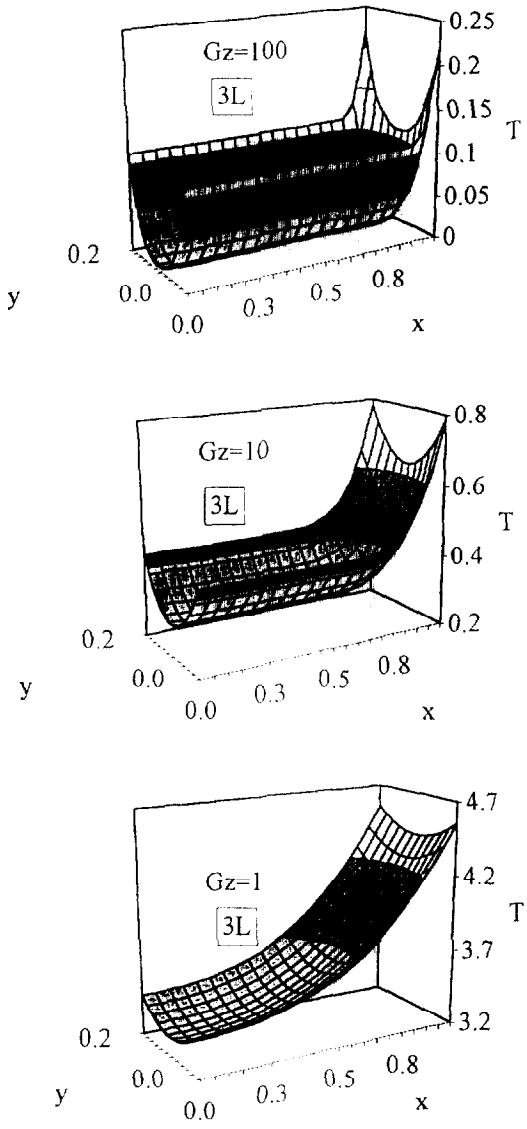

Fig. 3. Temperature distribution in the thermal entrance length, 3L version.

tribution for the 2S and 2L versions, respectively; the minimum occurs on the straight line $x = 0.5$ (Fig. 7) and $y = \beta/2$ (Fig. 8) of the cross section. The temperature difference between the centre and the heated walls is very remarkable near the inlet section, but it is progressively smoothed as the fluid approaches the fully developed region.

The thermal entrance length and the Nusselt numbers are very easily determined, in fact the numerical integration of equation (13) and the numerical solution to equation (14) are very inexpensive in terms of computational time. In Fig. 9 the thermal entrance length is sketched as a function of the aspect ratio; it is a monotonically increasing function of β for the 1L and 2L versions, starting from the typical values of the infinite parallel plates, i.e. 0.064515 for one heated wall, and 0.016129 for two heated walls, as discussed in [4], and reaching its maximum for the square duct. Quite different is the trend of L_{th} for the other boundary conditions; in the range $0.1 < \beta < 1$ the thermal entrance length is a decreasing function of β, except the 3S condition. In fact this version is very similar to the four heated walls condition up to $\beta = 0.6$, then its thermal entrance length reaches a minimun and increases to the square duct value. It is very interesting to point out that, in the analysis of the developing temperature profile in slug flow, a very flat rectangular duct can be approximated as infinite parallel

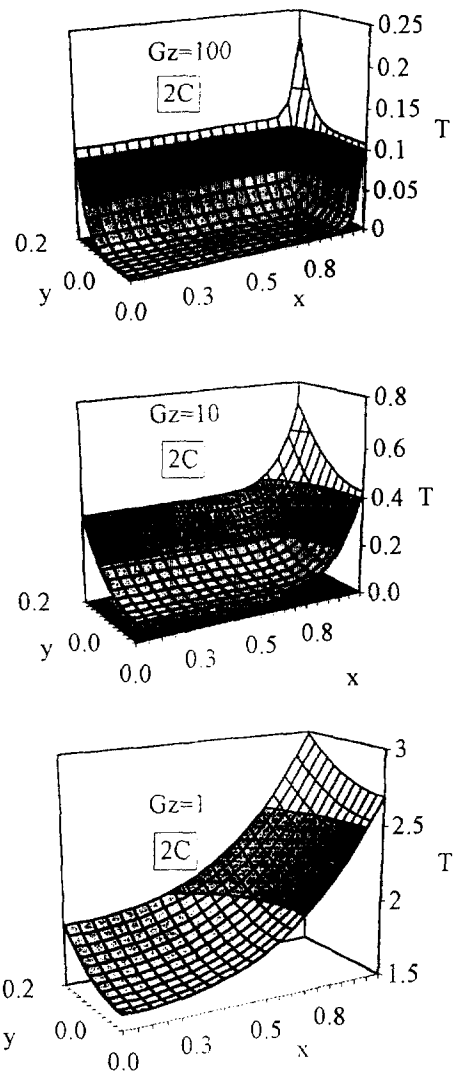

Fig. 4. Temperature distribution in the thermal entrance length, 2C version.

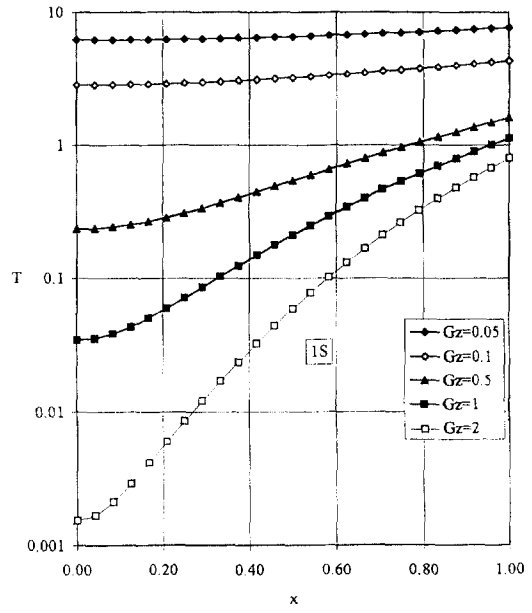

Fig. 5. Temperature distribution in the thermal entrance length, 1S version.

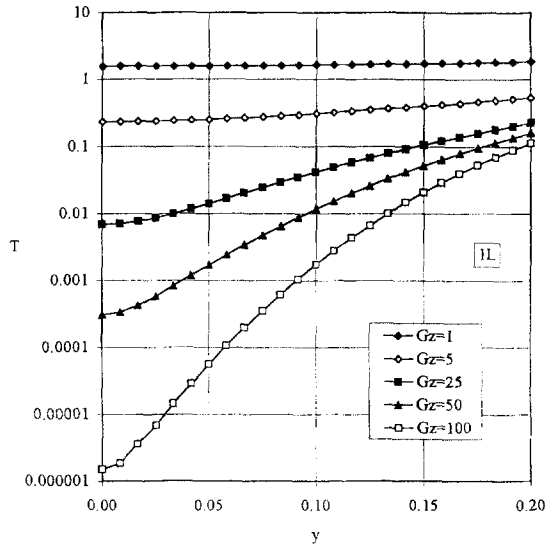

Fig. 6. Temperature distribution in the thermal entrance length, 1L version.

plates only in the frame of the 1L (one heated wall) and 2L (two heated walls) versions, all the other versions giving thermal entrance lengths very different from the typical slab values, in the limit of $\beta \to 0$.

Equation (11) in the limit of $z \to \infty$ provides the fully developed Nusselt numbers, they have been evaluated and reported in Fig. 10 as a function of β; they perfectly agree with the available data quoted in literature [2, 3]. One can see how the trend of the Nusselt number depends on the considered version; in fact for the boundary conditions 1L, 2L, and 3L the established Nusselt number decreases with β, while increases for the 1S, 2S, and 3S versions, and remains constant for the 2C and 4 versions. In the limit of $\beta \to 0$, the fully established Nusselt number tends to 0 for the 1S and 2S versions, to 3 for the 2C and 3S versions, to 6 for the 4, 1L, and 3L versions, to 12 for the 2L version. It is worth remembering that the Nusselt numbers for slug flow between infinite parallel plates is 12 for two heated walls, and 6 for one heated wall [2]. Consequently only the 2L version of the rectangular duct reproduces, in the limit of $\beta \to 0$, the slab with two heated walls, while the 4, 3L, and 1L versions reproduce (in the same limit) the slab with only one heated wall.

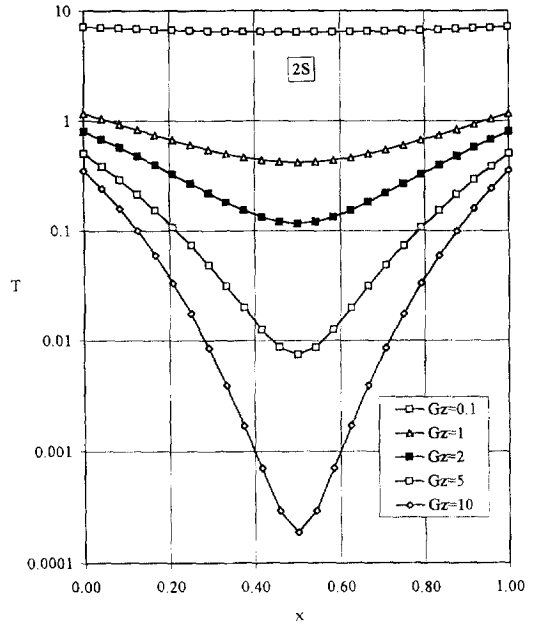

Fig. 7. Temperature distribution in the thermal entrance length, 2S version.

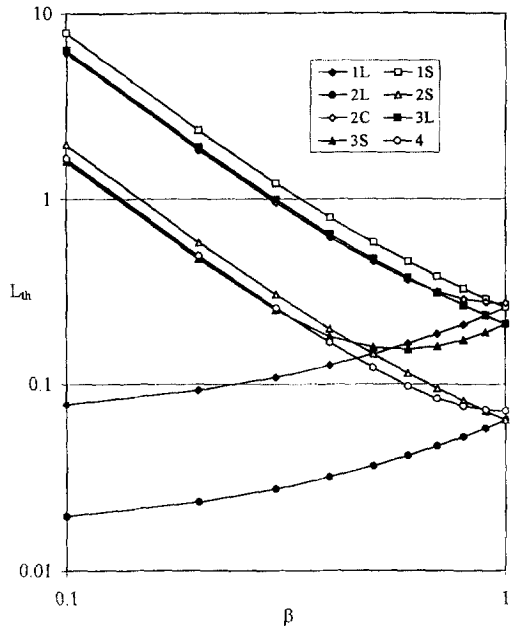

Fig. 9. The thermal entrance length as a function of the aspect ratio.

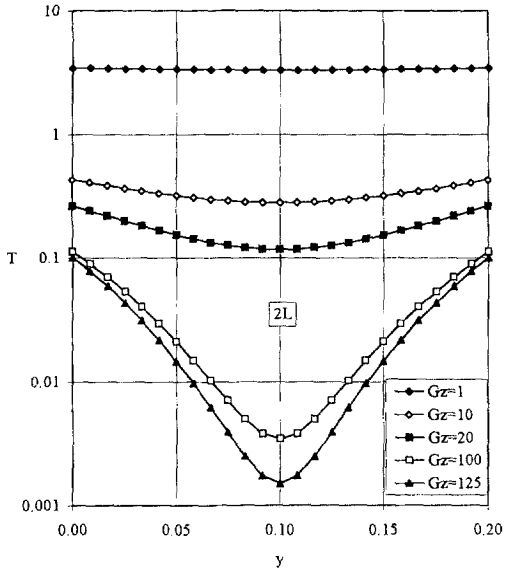

Fig. 8. Temperature distribution in the thermal entrance length, 2L version.

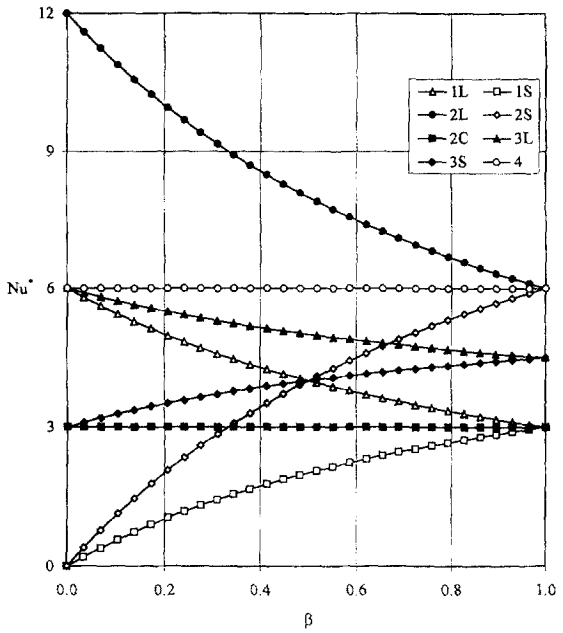

Fig. 10. Fully developed Nusselt number as a function of the aspect ratio.

The developing Nusselt numbers depend on two parameters: the longitudinal co-ordinate (or the Graetz number) and the aspect ratio. An accurate investigation is presented in [7], related only to the 1S, 1L, 2S, and 2L versions. Introducing the co-ordinate $z_{th} = z/L_{th}$ a very interesting peculiarity comes out: the thermal entrance lengths are very simple functions of the aspect ratio and the developing Nusselt ratio $Nu(z_{th})/Nu^*$ is the same function of z_{th} for any version and does not depend on the aspect ratio. No available data exists in literature concerning the remaining H2 versions; resorting to equation (11) the developing Nusselt numbers for these versions

Table 2
Ratio between the developing and the established Nusselt numbers, 2C version

β	$z_{th} = 0.1$	$z_{th} = 0.2$	$z_{th} = 0.3$	$z_{th} = 0.4$	$z_{th} = 0.5$	$z_{th} = 0.6$	$z_{th} = 0.7$	$z_{th} = 0.8$	$z_{th} = 0.9$	$z_{th} = 1$
1	2.125	1.612	1.396	1.275	1.198	1.146	1.110	1.083	1.064	1.05
0.9	2.115	1.606	1.392	1.272	1.196	1.145	1.109	1.083	1.064	1.05
0.8	2.081	1.585	1.377	1.262	1.189	1.140	1.106	1.081	1.063	1.05
0.7	2.014	1.544	1.349	1.242	1.176	1.131	1.101	1.078	1.062	1.05
0.6	1.909	1.481	1.308	1.215	1.158	1.121	1.094	1.075	1.061	1.05
0.5	1.772	1.404	1.262	1.188	1.143	1.112	1.090	1.073	1.060	1.05
0.4	1.623	1.336	1.231	1.174	1.137	1.110	1.089	1.073	1.060	1.05
0.3	1.490	1.299	1.221	1.171	1.136	1.109	1.089	1.073	1.060	1.05
0.2	1.424	1.293	1.220	1.171	1.136	1.109	1.089	1.073	1.060	1.05
0.1	1.420	1.293	1.220	1.171	1.136	1.109	1.089	1.073	1.060	1.05

Table 3
Ratio between the developing and the established Nusselt numbers, 3L version

β	$z_{th} = 0.1$	$z_{th} = 0.2$	$z_{th} = 0.3$	$z_{th} = 0.4$	$z_{th} = 0.5$	$z_{th} = 0.6$	$z_{th} = 0.7$	$z_{th} = 0.8$	$z_{th} = 0.9$	$z_{th} = 1$
1	1.756	1.395	1.256	1.184	1.140	1.110	1.089	1.072	1.060	1.05
0.9	1.682	1.359	1.239	1.176	1.136	1.109	1.088	1.072	1.060	1.05
0.8	1.610	1.330	1.227	1.171	1.135	1.108	1.088	1.072	1.060	1.05
0.7	1.541	1.308	1.221	1.170	1.134	1.108	1.088	1.072	1.060	1.05
0.6	1.483	1.296	1.218	1.169	1.134	1.108	1.088	1.072	1.060	1.05
0.5	1.442	1.293	1.218	1.169	1.134	1.108	1.088	1.072	1.060	1.05
0.4	1.423	1.292	1.218	1.169	1.134	1.108	1.088	1.072	1.060	1.05
0.3	1.419	1.291	1.217	1.169	1.134	1.108	1.088	1.072	1.060	1.05
0.2	1.419	1.291	1.217	1.169	1.134	1.108	1.088	1.072	1.060	1.05
0.1	1.419	1.291	1.217	1.169	1.134	1.108	1.088	1.072	1.060	1.05

Table 4
Ratio between the developing and the established Nusselt numbers, 3S version

β	$z_{th} = 0.1$	$z_{th} = 0.2$	$z_{th} = 0.3$	$z_{th} = 0.4$	$z_{th} = 0.5$	$z_{th} = 0.6$	$z_{th} = 0.7$	$z_{th} = 0.8$	$z_{th} = 0.9$	$z_{th} = 1$
1	1.756	1.395	1.256	1.184	1.140	1.110	1.089	1.072	1.060	1.05
0.9	1.834	1.436	1.279	1.197	1.147	1.114	1.090	1.073	1.060	1.05
0.8	1.923	1.487	1.311	1.216	1.158	1.120	1.094	1.075	1.061	1.05
0.7	2.011	1.540	1.346	1.239	1.173	1.129	1.099	1.078	1.062	1.05
0.6	2.081	1.583	1.375	1.259	1.187	1.138	1.104	1.080	1.063	1.05
0.5	2.113	1.603	1.389	1.269	1.194	1.143	1.108	1.082	1.064	1.05
0.4	2.066	1.574	1.369	1.255	1.184	1.136	1.103	1.080	1.063	1.05
0.3	1.890	1.468	1.298	1.208	1.153	1.117	1.092	1.074	1.060	1.05
0.2	1.607	1.328	1.226	1.171	1.134	1.108	1.088	1.072	1.060	1.05
0.1	1.422	1.291	1.218	1.169	1.134	1.108	1.088	1.072	1.059	1.05

Table 5
Ratio between the developing and the established Nusselt numbers, 4 version

β	$z_{th} = 0.1$	$z_{th} = 0.2$	$z_{th} = 0.3$	$z_{th} = 0.4$	$z_{th} = 0.5$	$z_{th} = 0.6$	$z_{th} = 0.7$	$z_{th} = 0.8$	$z_{th} = 0.9$	$z_{th} = 1$
1	2.098	1.592	1.380	1.263	1.189	1.139	1.105	1.080	1.063	1.05
0.9	2.086	1.584	1.375	1.259	1.186	1.137	1.104	1.080	1.062	1.05
0.8	2.049	1.561	1.359	1.248	1.178	1.132	1.101	1.078	1.062	1.05
0.7	1.981	1.520	1.331	1.229	1.166	1.124	1.096	1.076	1.061	1.05
0.6	1.872	1.456	1.290	1.202	1.149	1.114	1.090	1.073	1.060	1.05
0.5	1.740	1.385	1.250	1.180	1.137	1.108	1.087	1.071	1.059	1.05
0.4	1.597	1.324	1.224	1.168	1.133	1.106	1.087	1.071	1.059	1.05
0.3	1.476	1.294	1.217	1.167	1.132	1.106	1.087	1.071	1.059	1.05
0.2	1.421	1.289	1.216	1.167	1.132	1.106	1.087	1.071	1.059	1.05
0.1	1.418	1.289	1.216	1.167	1.132	1.106	1.087	1.071	1.059	1.05

too can be easily calculated. Tables 2–5 show the Nusselt ratio for these remaining versions (2C, 3L, 3S, 4) as a function of both the aspect ratio and the axial co-ordinate z_{th}; obviously the Nusselt ratio is always 1.05 for $z_{th} = 1$.

For any cross section (z = constant) of the thermal entry region, the Nusselt number is a monotonically increasing function of β for all the versions, except the 3S condition (Table 4), where the Nusselt number at first increases with β reaching its maximum at $\beta = 0.5$, then decreases to the square duct value.

A comparison between these numerical results and the graphical data quoted in literature can be performed only in the square duct with four heated walls, page 293 in [2], the agreement is quite satisfactory.

5. Concluding remarks

The paper has analysed the thermal behaviour of a slug flow in the thermal entrance region of rectangular ducts, in H2 boundary conditions. The 3-D temperature distribution has been analytically determined as a simple series of cosinusoidal functions of x and y, and linear and exponential functions of z; the coefficients of the series depend on the different combinations of heated and adiabatic walls. The thermal entrance lengths are numerically calculated and shown in a graph as a function of the aspect ratio. At last the developing Nusselt numbers have been calculated as functions of both the duct aspect ratio and the Graetz number, they are presented in exhaustive Tables.

Acknowledgement

This research was financially supported by the Italian C.N.R. and M.U.R.S.T.

References

[1] Fraas AP. Heat Exchanger Design. Wiley, New York, 1989.
[2] Hartnett JP, Kostic M. Heat transfer to Newtonian and non-Newtonian fluids in rectangular ducts. Ed. J. C. Hartnett. Academic Press, New York. In Advances in Heat Transfer 1989;19.
[3] Gao SX, Hartnett JP. Analytical Nusselt number predictions for slug flow in rectangular ducts. International Communications in Heat and Mass Transfer 1994;20:751–760.
[4] Spiga, M, Morini GL. Nusselt numbers in laminar flow for H2 boundary conditions. International Journal of Heat and Mass Transfer 1996;39:1165–1174.
[5] Javeri V. Analyses of laminar thermal entrance region of elliptical and rectangular channels with Kontorowich method. Wärme und Stoffübertragung 1976;9:85–90.
[6] Javeri V. Laminar heat transfer in a rectangular channel for the temperature boundary conditions of the third kind. International Journal of Heat and Mass Transfer 1978:21:1029–1034.
[7] Spiga M, Morini GL. The thermal entrance length problem for slug flow in rectangular ducts. ASME Journal of Heat Transfer 1996;118:979–982.
[8] Özisik MN. Boundary Value Problems of Heat Conduction. Dover Publication Inc., New York, 1989.